JOURNAL OF CATALYSIS 155, 106–116 (1995)

Oxidative Coupling of Methane over Lanthana Catalysts

II. A Mechanistic Study Using Isotope Transient Kinetics

S. Lacombe,* H. Zanthoff,† and C. Mirodatos*,[1]

*Institut de Recherches sur la Catalyse, 2 Avenue Albert Einstein, 69626 Villeurbanne Cedex, France; and †Lehrstuhl für Technische Chemie, Ruhr-Universität Bochum, Bochum D-44780, Germany

Received September 24, 1994; revised March 20, 1995

The elementary steps dealing with the methane and oxygen activation in the reaction of oxidative coupling of methane (OCM) over lanthana catalysts have been investigated by means of state-of-the-art transient kinetic techniques. Methane and oxygen activation over lanthana catalysts are shown to combine reversible and irreversible steps, parallel for methane and consecutive for oxygen. In both processes, the surface residence time of activated species per active site is found to be below the time resolution of 1 ms, characteristic of the temporal analysis of products reactor. Evidence of a strong interaction between gaseous and lattice oxygen and of an inhibiting effect of carbon dioxide on both methane and oxygen activation is also provided. Specific sites pertaining to each of these routes are proposed, accounting for the various kinetic effects which are observed under the OCM conditions. © 1995 Academic Press, Inc.

INTRODUCTION

After a decade of intense research devoted to the reaction of oxidative coupling of methane (OCM), it is now accepted that the mechanism involves a large number of elementary steps, between gas and surface, on the surface, or in the gas phase, as stressed in the most recent reviews on the topic (1–5). Among these steps, the initial activation of the reactants is of prime importance since it has been shown to monitor the overall kinetics, at least for moderate conversion, when the further conversion of products is still reduced (5).

As far as methane is concerned, although the formation of methyl radicals has been convincingly established by various methods (2, 6, 7), direct information on the initial activation step is still missing or controversial. It is not clear whether it proceeds directly on an electrophilic oxygen atom (type O^-) via a homolytic cleavage of the C–H bond, producing a methyl radical CH_3 and a surface OH group (8), or implies an initial heterolytic dissociation on a lattice site $\{M^{n+}O^{2-}\}$ and subsequent electron abstraction on a lattice defect in order to form the methyl radical (9). Alternatively, it has also been proposed (10) that at low temperature, gaseous oxygen may directly react with the carbanion CH_3^- formed by a heterolytic dissociation of methane to give a methyl radical. The first step of methane activation likewise addresses the question of CH_4 adsorption under reaction conditions. Several transient studies led to the conclusion that almost no methane was stabilised on the surface under reaction conditions (11–14).

As far as oxygen activation is concerned, the strong interaction of gaseous oxygen with the lattice oxygen has been attested to by several studies (11, 12, 15). However, the identification of the actual active site, as well as the mode of adsorption (dissociative or nondissociative), remains a matter of discussion. Buyevskaya *et al.* (14) reached the conclusion that the kind of active site, i.e., lattice or adsorbed oxygen, strongly depends on the catalyst.

The formation of C_2 hydrocarbons has been shown to originate from the coupling of two methyl radicals, most likely in the presence of a third body for energy dissipation (16, 17). However, no direct and unambiguous evidence has yet been obtained to determine whether the coupling step occurs on the catalyst surface or in the gas phase. Observations of simultaneous changes in CH_3 radical and C_2H_6 concentration along a tubular Sr/La_2O_3 reactor (8) or in a *temporal analysis of products* (TAP) reactor loaded with Sm_2O_3 (14) and other studies on the CH_4/CD_4 reaction (18) tend to support the assumption that the coupling step is essentially a gas phase reaction.

Clear kinetic H/D isotopic effects (KIE) have been observed in the OCM reaction by comparing reactivities of CH_4 and CD_4 to C_2 hydrocarbons (17, 19, 20). From these effects, it has been proposed that the initial C–H bond cleavage of methane was the rate determining step (RDS) on the basis of theoretical calculations of KIE. However, other RDS involving the activation of O–H bonds, which

[1] To whom correspondence should be addressed.

0021-9517/95 $12.00

would lead to similar KIE (19–21), may also be considered. Concerning the formation of CO_x, the RDS are still controversial. In a recent review, Lunsford (1) proposed that several RDS could actually control the overall process, depending on the oxygen partial pressure.

In order to answer some of the still open questions dealing with the OCM mechanism, we have studied a model catalyst stable and active, (9, 22), which is particularly effective for generating methyl radicals (23), namely unsupported lanthanum oxide. The first part of the study (22) was devoted to a combined approach of (i) the surface characterisation under the reaction conditions and (ii) the kinetics of the unselective route leading to the formation of CO_2. Evidence of specific sites located on the edges of the outer planes of the crystal was provided, and the surface oxidation of methyl radicals into CO_2 on these sites was kinetically described. The aim of the present part of the study was to determine an overall mechanistic process of the OCM reaction, focusing on the activation of methane and oxygen, considered first separately, then under coactivation conditions, i.e., under the OCM conditions. The eventual role played by CO_2 as a possible coreactant (in competition with the proper reactants) or as a poison was also investigated. Techniques allowing evaluation of the actual concentration of the activated species on the catalyst together with their mean residence time on the surface were implemented, such as exchange reactions (CH_4/CD_4, $^{16}O_2/^{18}O_2$), stationary-state isotopic transients, and fast pulsed transients carried out in a TAP reactor.

EXPERIMENTAL

Catalyst preparation. The lanthanum oxide catalyst was prepared from lanthanum nitrate $La(NO_3)_3$, $6H_2O$ supplied by Rhône-Poulenc, with the following procedure: (i) decomposition of the nitrate under air at 500°C for 3 h, (ii) crushing of the powder and sieving to 200–300 μm, and (iii) calcination under pure oxygen at 650°C for 2 h (flow rate of 0.5 cm^3/s). The lanthanum oxide samples were characterised during (*in situ* measurements) and after OCM reaction in order to account for the morphological and structural changes induced by the reaction, as reported in Ref. (22). Thus, the BET surface area after reaction at 750°C under $CH_4/O_2/He$ (8/4/88, 0.5 cm^3/s) reacting mixture was 2.4 m^2/g.

Steady-state isotopic transient kinetics. The isotopic transient experiments under steady-state conditions were carried out by switching abruptly with an automated four-way valve located just before the reactor from a nonlabelled feeding mixture $^{12}CH_4/^{16}O_2/He$ (8/4/88, 0.5 cm^3/s) to either $^{13}CH_4/^{16}O_2/He$ or $^{12}CH_4/^{18}O_2/He$ with the same flowrate and composition. Details on the technique are reported elsewhere (22, 25).

Steady-state isotopic exchange reaction. The CH_4/CD_4 equilibration, i.e., the isotopic exchange of an equimolecular mixture of CH_4 and CD_4 fed into a flow microreactor, was investigated under various conditions on about 20 mg of lanthanum oxide: $CH_4/CD_4/He$ = 6/6/88, 0.5 cm^3/s; $CH_4/CD_4/O_2/He$ = 6/6/6/82, 0.5 cm^3/s; $CH_4/CD_4/CO_2/He$ = 6/6/20/68, 0.5 cm^3/s. In order to avoid any overlapping of the methane isotopes (CH_4, CH_3D, CH_2D_2, CHD_3, and CD_4) with other compounds or fragments (H_2O, HDO, and D_2O), GC/MS coupling was used for gas analysis. Data were corrected for fragmentation and naturally occurring isotopes and sensitivity factors interpolated as detailed in Ref. (25). The degree of exchange was calculated from the ratio of the actual number of exchanged H and D atoms to the number of exchanged atoms in the statistical distribution, varying therefore between 0 and 1.

Catalytic tests in a TAP reactor. Two hundred milligrams of calcined and sieved (200–300 μm) catalyst was introduced into a TAP inconel reactor between two layers of quartz (24) and pretreated at 650°C for 2 h under continuous oxygen flow (400 Torr in the continuous solenoid valve, reaction chamber maintained under vacuum).

The experiments consisted of pulsing various reacting mixtures: CH_4/Ar 60/40, O_2/Ar 90/10, $^{18}O_2/Ne$ 33/66, $^{16}O_2/^{18}O_2/Ne$ 17/17/66, $CH_4/O_2/He$ 60/30/10. Different types of pulse sequence were applied: these were either single pulses of one given mixture or subsequent pulses of oxygen, then methane, with an adjustable time interval between the two pulses. In all cases, 10 sequences were accumulated for maximising the signal/noise ratio, after 4 sequences for stabilisation. The pulses were either of low intensity (10^{15} molecules per pulse) or high intensity (2×10^{16} molecules per pulse). Each signal was smoothed and the resulting peaks integrated. The recorded mass units were 15 and 16 for methane, 17 for water, 26 or 27 for ethylene after correction for the ethane contribution, 28 for carbon monoxide after correction for the ethane and ethylene contribution, 30 for ethane, 32 for oxygen (plus 34 and 36 for labelled oxygen), and 44 for carbon dioxide. By analysing the ratio of 15 amu to 16 amu provided by the mass spectrometer, in a way similar to that used by Buyevskaya *et al.* (14), the presence of methyl radicals at the reactor outlet as a product of the OCM reaction was quantified. In order to compare several sets of experiments, the outlet signals were corrected for pulse intensity fluctuation. An inert gas (argon or neon) was used as an internal standard. Furthermore, each reacting mixture was pulsed at 150°C, where no adsorption nor storage of reactant occurs. With the inert gas peak as a reference, the actual amount of methane and/or oxygen admitted onto the catalyst could then be determined at the different temperatures.

For the simple case of oxygen/inert gas or methane/inert gas pulses admitted in the absence of methane, i.e., when the output pulse shape depends only on the surface adsorption/desorption and transport phenomena, an absolute first moment (m_1/m_0) was calculated, corresponding to the mean residence time of the concerned species in the whole system (24). The value for the inert gas represented the time needed to cross the system without any chemical interaction. Assuming a Knudsen regime, this time was proportional to the reverse of the Knudsen diffusion coefficient, i.e., to the square root of the mass unit. Accordingly, from the inert gas residence time it was possible to evaluate the time of flight of oxygen or methane throughout the reactor excluding any chemical interaction. The difference between this calculated time and the experimental one provided an evaluation of the mean residence time of the considered gas on the catalyst surface. The assumption of a Knudsen regime was verified for low-intensity pulses admitted either on an inert material (quartz powder of granulometry close to that of the tested catalysts) or on the proper catalyst, but at room temperature when no chemical activation is expected to occur: the mean residence time of the different pulsed gases (CH_4, O_2, and Ar) was found to be strictly proportional to the square root of their molecular weight. This indicated unambiguously that the gases were crossing the TAP reactor without significant interaction or collision between gaseous species (24). With high-intensity pulses, a more viscous regime was achieved, tending to the molecular regime corresponding to experiments carried out at one atmosphere in a dynamic flow reactor.

RESULTS

Methane/Surface Interaction

SSITK experiments. SSITK experiments were carried out by tracing the carbon atom of methane in the presence of oxygen, switching between $^{12}CH_4/O_2/He$ and $^{13}CH_4/O_2/He$ either at 620°C (Fig. 1) or at 750°C. Whatever the temperature, the response curve of methanes (labelled or unlabelled) was similar when the reactor was filled either with quartz (inert material under the prevailing conditions) or with lanthana. This result indicates that no reversibly adsorbed methane accumulates on the lanthana surface under reaction conditions. However, this should be considered with care since it corresponds to the experimental limits of the transient method regarding time resolution (around 0.1 s). TAP experiments, better adapted to short residence times, were carried out to ascertain this point.

TAP experiments. TAP experiments on methane adsorption were carried out by single methane pulses of low intensity in the absence and presence of oxygen. In the absence of oxygen (Fig. 2a, at 650°C), the surface of the output pulse of methane was always identical to the surface of the input pulse, attesting to the absence of any uptake of methane by the catalyst. The mean residence time of methane on the surface, calculated from these experiments, was around 0.004 s at 650°C, i.e., a figure close to the limit of the TAP time resolution. In other words, methane behaved mostly as an inert gas towards the lanthana catalyst. In the presence of oxygen (at 650°C in Fig. 2b), the output pulse was indeed smaller due to the reaction of part of the methane with oxygen, but no significant curve shape, i.e., no change in methane residence time, was observed. This tends to confirm that no measurable accumulation of reversible methane occurred on the surface under OCM conditions, as anticipated from SSITK experiments.

The absence of methane uptake by the catalyst under OCM conditions was also confirmed by volumetric measurements, as reported elsewhere (26).

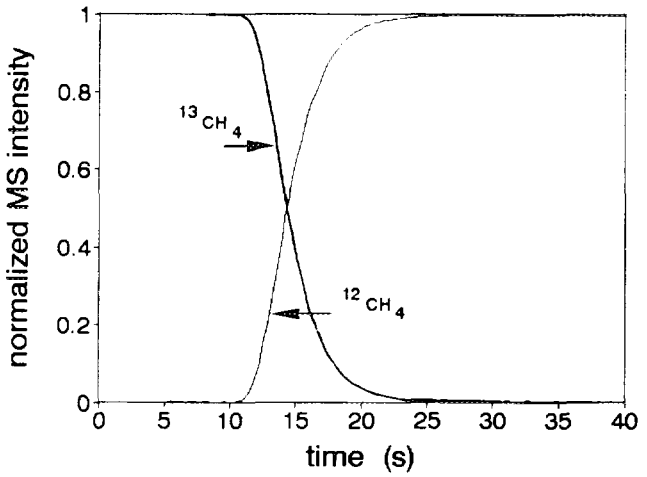

FIG. 1. Normalised SSITK curves for the isotopic switch $^{13}CH_4/O_2/He \rightarrow {}^{12}CH_4/O_2/He$ at 620°C either in the absence of catalyst or over La_2O_3.

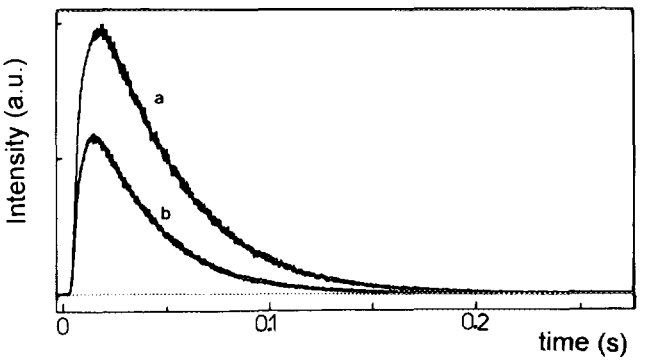

FIG. 2. TAP response to a CH_4 (a) and a CH_4/O_2 (b) single pulse at 650°C over La_2O_3.

Reversible Activation of Methane

The reaction of CH_4/CD_4 equilibration under a steady-state regime was investigated in order to evaluate the extent of reversible methane activation and the influence of oxygen and carbon dioxide. The degrees of isotopic exchange obtained are summarised in Table 1. Several features can be outlined:

(i) Whatever the experimental conditions, a noticeable isotope exchange occurred between CH_4 and CD_4, always increasing with temperature. The products of exchange were essentially CH_3D and CHD_3 at low extent of equilibration, indicating that only one hydrogen or deuterium atom was exchanged per adsorption–desorption cycle.

(ii) In the presence of oxygen, i.e., under OCM conditions, the CH_4/CD_4 equilibration rate decreased significantly. Under these conditions, a large part of the methanes were converted into OCM products, which resulted both in a lower partial pressure of methane and in a partial pressure of CO_2 between 1 and 2 kPa in the catalytic bed. The isotopic composition of the OCM products was found in accordance with the expected mechanism assuming the coupling of two methyl radicals. Thus, a predominant production of C_2H_6, $C_2H_3D_3$, and C_2D_6 was observed for ethanes produced at low conversion, as already reported elsewhere (18, 19, 27). It can also be mentioned that the light methane was more converted into OCM products than the deuterated one, attesting to a marked kinetic isotopic effect, as generally observed for this reaction (19–21).

(iii) When CO_2 was added to the feeding mixture at 750°C, the extent of equilibration was divided by around 25, which clearly demonstrates that CO_2 acts as a poison towards methane equilibration.

TABLE 1

Results of CH_4/CD_4 Equilibration as a Function of Temperature and Operating Conditions

Reacting mixture	T (°C)	p_{CO_2} (kPa)	$X_{CH_4+CD_4}$ (%)	Y_{C_2} (%)	α (%)
$CH_4/CD_4/He$	650	—	—	—	4.5
	700	—	—	—	12.2
	750	—	—	—	24.6
$CH_4/CD_4/O_2/He$	650	1.1	14.0	1.4	3.3
	700	1.5	25.9	7.1	7.7
	750	1.9	34.2	12.4	20.6
$CH_4/CD_4/CO_2/He$	750	20	—	—	3.8

Note. $X_{CH_4+CH_4}$, conversion of methanes into C_2 and CO_x; Y_{C_2}, C_2 yield; α, degree of isotopic exchange.

Irreversible Activation of Methane

Having considered the effect of CO_2 on the reversible activation of methane via the CH_4/CD_4 equilibration, this effect has also been investigated for the irreversible activation of methane by following the change in the rate of methane conversion into OCM products as a function of the pressure of CO_2 added to the reacting feed at 750°C (Fig. 3). It is clear that carbon dioxide also inhibits the irreversible activation of methane in the OCM reaction, as already assessed by Roos *et al.* on Li/MgO (28). However, this effect appears much less drastic than the inhibiting effect on the reversible activation of methane.

Oxygen Activation in the Absence of Methane

SSITK experiments. SSITK experiments were carried out by switching from $^{16}O_2$ to $^{18}O_2$ at the microreactor inlet in the absence of reaction with methane at 750°C (Fig. 4). It was first checked that no oxygen exchange occurred in the absence of catalyst (dotted lines in the left-hand part of Fig. 4). In the presence of catalyst, the $^{16}O_2$ concentration in the effluent came down at a slower rate with time after the switch was made to $^{18}O_2$ in the gas phase. One can notice also the intermediate formation of the mixed oxygen product $^{16}O^{18}O$ which resulted from the isotopic exchange between the two $^{16}O_2$ and $^{18}O_2$ flows. The concentrations of the three output components $^{16}O_2$, $^{16}O^{18}O$, and $^{18}O_2$ were very close to the statistical equilibrium at any time of the experiment. Thus, the average degree of exchange (which was calculated from the ratio of the actual number of exchanged O atoms to the number of exchanged O atoms in the statistical distribution) was around 98% under the present conditions.

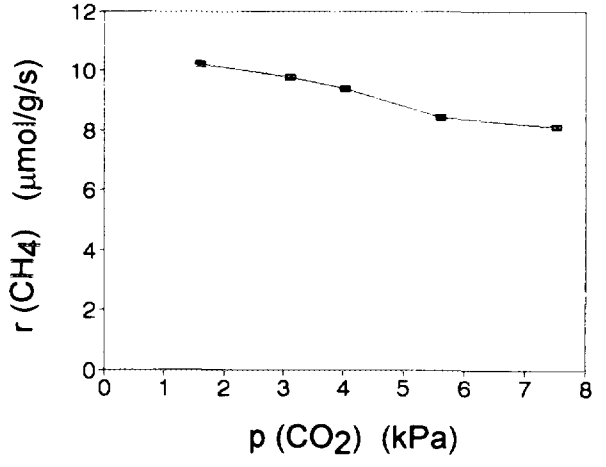

FIG. 3. Rate of CH_4 conversion as a function of the CO_2 partial pressure added to the reacting $CH_4/O_2/Ar$ mixture in an atmospheric recycling reactor (T = 750°C, p_{CH_4} = 10.1 kPa, p_{O_2} = 1.1 kPa).

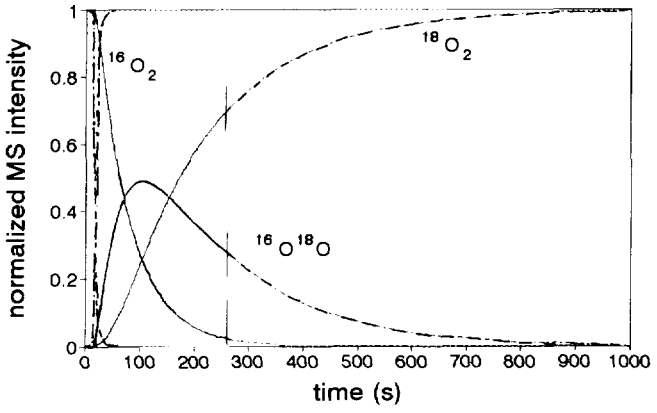

FIG. 4. Normalised SSITK curves for the isotopic switch $^{16}O_2$/He → $^{18}O_2$/He in the absence of methane at 750°C over La_2O_3 (m = 17.3 mg). The dotted lines after 260 s are modelled curves on the basis of the experimental ones. The dotted lines in the left-hand part of the figure correspond to the switch in the absence of catalyst.

TAP experiments with single pulses of unlabelled oxygen. By admitting single pulses of oxygen onto the catalyst at different temperatures (from 150 to 750°C), it was observed that the surface area of the pulses was strictly constant and equal to the surface area observed in the absence of catalyst. This result demonstrates that no irreversible oxygen uptake occurred on the lanthana catalyst under OCM temperature conditions. The mean residence time of the pulsed oxygen molecules on the catalyst surface was calculated for various operating conditions (Table 2). As one can see, the mean residence time, whatever the temperature, tended to increase with the catalyst loading, as qualitatively observed through peak broadening. This observation suggests that readsorption–redesorption equilibria occurred throughout the catalytic bed, leading to a kind of chromatographic effect.

TABLE 2

Mean Residence Time of Oxygen in TAP Reactor for O_2/Ar (90%/10%) Pulses of Low Intensity, as a Function of Temperature (T) and Catalyst Weight (m_{cat})

m_{cat}(mg)	T(°C)	τ_s(s)
200	650	0.44
	750	0.23
50	650	0.07
	750	0.04

Note. τ_s, mean residence time on the catalyst surface.

An attempt to quantify the proper residence time of activated oxygen on the surface during a single adsorption–desorption process was made by extrapolating to zero loading the mass of catalyst. Actually this led to a slightly negative value, indicating that the elementary residence time of activated oxygen on the surface was below the TAP time resolution, i.e., below 1 ms.

TAP experiments with single pulses of labelled oxygen. $^{18}O_2$/Ne single pulses were admitted onto the catalyst after calcination under flowing $^{16}O_2$, i.e., when all the oxygen atoms of the solid were expected to be ^{16}O (except the negligible fraction of naturally occurring isotopes). Three output pulses of $^{18}O_2$, $^{16}O^{18}O$, and $^{16}O_2$ were recorded, the first two appearing as rather small and sharp peaks, the third one being much larger and broader (Fig. 5). As expected from the previous experiment with unlabelled oxygen, the total surface area of the three output peaks was equal to the surface area of the input $^{18}O_2$ pulses, confirming that no oxygen was irreversibly adsorbed. The amount of output $^{18}O_2$ and $^{16}O^{18}O$ represented only 5% of the total oxygen input at 650°C and 1.7% at 750°C. This means that the $^{18}O_2$ input molecules were almost completely incorporated into the large reservoir of lattice ^{16}O oxygen atoms of the catalyst.

The catalyst was then pretreated under $^{18}O_2$ by means of about 1400 consecutive pulses, equivalent to 3×10^{19} molecules, aiming at its enrichment in labelled oxygen. A $^{18}O_2$/Ne single pulse was then admitted onto the catalyst as done previously. The resulting output-labelled oxygen pulses are presented in Fig. 6 (full lines), together with the corresponding pulses obtained before the pre-enrichment (dashed lines); $^{16}O_2$ output pulses are omitted for the sake of clarity. As one can see, the effect of the $^{18}O_2$ pre-enrichment was to increase significantly the relative amount of output $^{18}O_2$ and $^{16}O^{18}O$ molecules (from 2.8 to 9.8% of the total oxygen output amount, by comparison with the experiment carried out without isotopic pre-en-

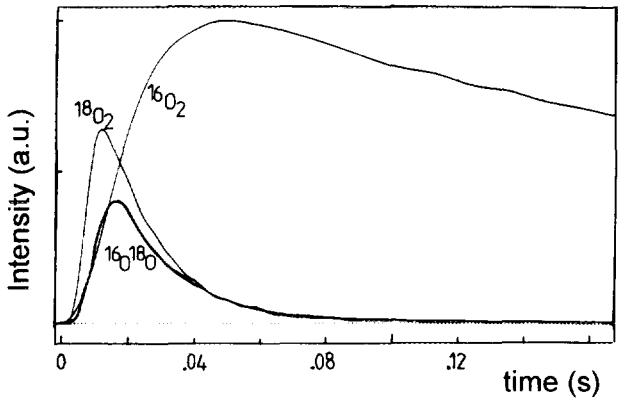

FIG. 5. TAP response to a $^{18}O_2$/He single pulse of low intensity (10^{15} molecules per pulse) at 650°C, after La_2O_3 calcination under $^{16}O_2$.

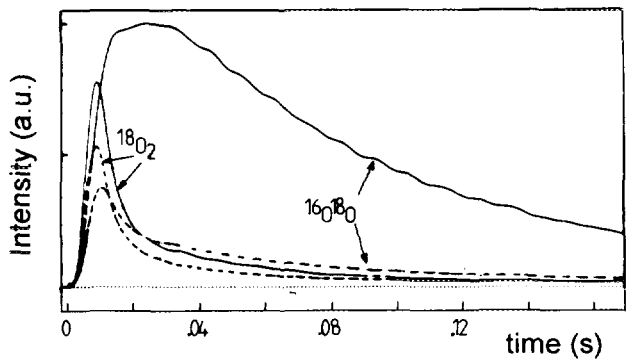

FIG. 6. TAP responses to a $^{18}O_2$/He single pulse of high intensity (2×10^{16} molecules per pulse) at 750°C, after $^{18}O_2$ pre-enrichment (full lines) or without pre-enrichment (dotted lines) of the lanthana catalyst. The $^{16}O_2$ output curves are not reported for sake of clarity.

richment). In Table 3, the mean experimental isotopic distribution at the reactor outlet is compared to the distribution calculated assuming a statistical mixing. The similarity of both experimental and calculated distributions demonstrates that all the gaseous oxygen molecules from the input pulse were adsorbed dissociatively and recombined in a statistical way. It is interesting now to determine whether the statistical mixing of the oxygen atoms was achieved by means of only a part of the lattice oxygen atoms (for instance surface and subsurface) or involved all the oxygen atoms of the catalyst. The mean isotopic composition of the lattice oxygen can be evaluated by assuming, in accordance with the previous experiment, that all the labelled oxygen molecules fed during the enrichment pretreatment were incorporated into the lanthana sample; this makes around 6×10^{19} ^{18}O atoms (evaluated from the number of $^{18}O_2$ pulses sent during the pretreatment), i.e., 5.1% of all the lattice oxygen atoms (as calculated on the basis of the lanthana particles model proposed in Ref. (22). Now the percentage of ^{18}O atoms in the gas phase at the reactor outlet is directly deduced from the experimental distribution of gaseous oxygen in Table 3: this makes 0.5 [8.7 + 2(1.1)] = 5.4%. It is thus observed that both ^{18}O contents in the gas phase and in the solid phase (considered as a whole) are very close. This result indicates that the isotopic mixing of all the oxygen atoms of the oxide was fast enough throughout the bulk for isotopic equilibrium between the gas and the solid phase to be achieved, without any surface enrichment.

TABLE 3

Experimental and Statistical Isotopic Distribution of Oxygen at the TAP Reactor Outlet after a Pulse of $^{18}O_2$ at 750°C

	Isotopic Distribution (%)	
Oxygen	Experimental	Statistical
$^{16}O_2$	90.2	89.4
$^{16}O^{18}O$	8.7	10.3
$^{18}O_2$	1.1	0.3

Effect of CO_2 on the Oxygen Activation

CO_2 being a major constituent of the OCM reaction (see Table 4), its specific effect on oxygen activation was investigated on the TAP system by comparing the shape of oxygen pulses admitted before and after a pretreatment of the lanthana catalyst under CO_2. Figure 7 reports the normalized outlet oxygen pulses of low intensity recorded before and after a CO_2 pretreatment at 750°C. Sharper peaks were observed after the CO_2 treatment (normalized as Figs. 7b and 7c); they corresponded to a significant decrease of the mean residence time of oxygen on the catalyst from 0.30 to 0.12 s for a catalyst loading of 200 mg. After 1 h treatment under vacuum at 750°C, the initial shape of the oxygen pulses was restored (Fig. 7d). The observed decrease in the mean residence time of oxygen on a CO_2 pretreated surface indicated a marked inhibition of the oxygen reversible activation. The slow disappearance of this inhibition effect under vacuum suggested that the interaction of CO_2 with the surface was unstable under the TAP vacuum conditions. Knowing that lanthana reacts easily with CO_2 to form surface carbonates which are slowly decomposed under vacuum at high temperature (22), it may be deduced that the inhibition effect on oxygen reversible activation after CO_2 treatment was due to carbonate formation.

TABLE 4

Catalytic Data Obtained at 750°C under (a) Pulsed Regime (TAP Reactor) and (b) Steady-State Regime (Dynamic Microreactor)

Reactor	TAP[a]		Dynamic[b]
Diffusion regime	Low intensity pulses Knudsen	High intensity pulses intermediate	Molecular
X_{CH_4} (%)	24	34	31
X_{O_2} (%)	99	91	61
S_{CH_3} (%)	68	18	–
$S_{C_2H_6}$ (%)	8	8	17
$S_{C_2H_4}$ (%)	0	16	19
S_{CO} (%)	27	15	13
S_{CO_2} (%)	(−3)[c]	(43)[c]	49

[a] Catalyst loading: 200 mg. Feed composition: $CH_4/O_2/Ar = 60/30/10$.
[b] Catalyst loading: 15.4 mg. Feed composition: $CH_4/O_2/He = 8/4/88$.
[c] Evaluated on the basis of a 100% carbon balance.

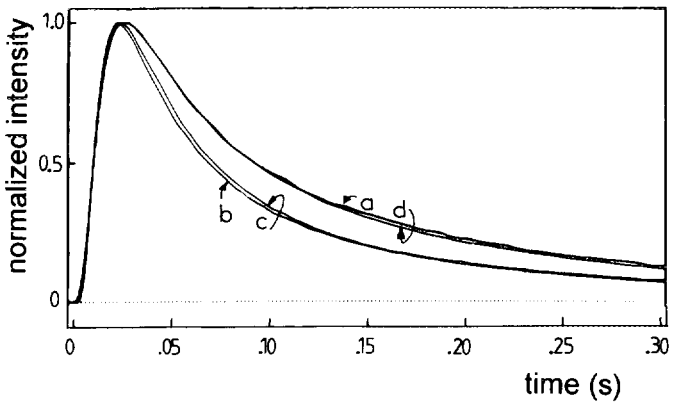

FIG. 7. Normalised TAP responses to a $^{16}O_2$ single pulse at 750°C, (a) after calcination under flowing $^{16}O_2$ at 750°C, (b) after 10 min CO_2 treatment at 750°C, (c) after 30 min CO_2 treatment at 750°C, and (d) after 60 min evacuation at 750°C.

Effect of the Reaction on the Oxygen Activation

Oxygen SSITK experiments. Oxygen SSITK experiments carried out in the presence of methane (i.e., switching from $^{16}O_2$ to $^{18}O_2$ under reaction conditions, Fig. 8) revealed the same type of curves as in the absence of methane (see Fig. 4 for comparison); however, a much lower intermediate formation of the mixed oxygen product $^{16}O^{18}O$ indicated that the isotopic exchange between the two $^{16}O_2$ and $^{18}O_2$ flows was slower under reaction conditions. Thus, the degree of isotopic exchange at 750°C was only 37% of the statistical equilibrium, instead of 98% in the absence of methane. By measuring this degree of isotopic exchange at various temperatures, the apparent activation energy for the oxygen exchange process was found to be 89 ± 5 and 98 ± 5 kJ/mol in the presence and absence of methane, respectively. These close values indicate that the OCM reaction which inhibited the rate of exchange did not significantly alter its mechanism.

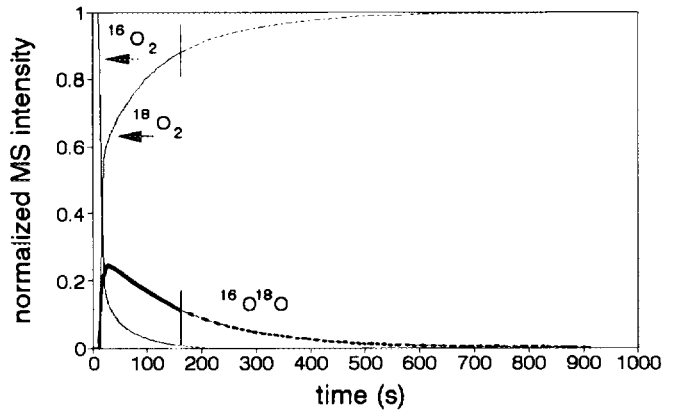

FIG. 8. Normalised SSITK curves for the isotopic switch $CH_4/^{16}O_2/He \rightarrow CH_4/^{18}O_2/He$ at 750°C over La_2O_3 (m = 17.3 mg). The dotted lines on the right are modelled curves on the basis of the experimental ones.

By integrating the SSITK curves in Fig. 8, then subtracting the surface area under the curves obtained without catalyst (providing the system response without any adsorption), the percentage of lattice oxygen atoms (^{16}O atoms) participating in the surface/gas phase equilibrium in the presence of methane was found to be ca. 6.5%. This corresponds to around the first six layers of lattice oxygen, considering the model of the lanthana particles proposed in Ref. (22).

Role of Gaseous Oxygen in the OCM Reaction

In order to estimate whether some delay was required between the oxygen activation and the methane conversion in the OCM process, pulses of oxygen and methane were sequentially admitted into the TAP reactor and the

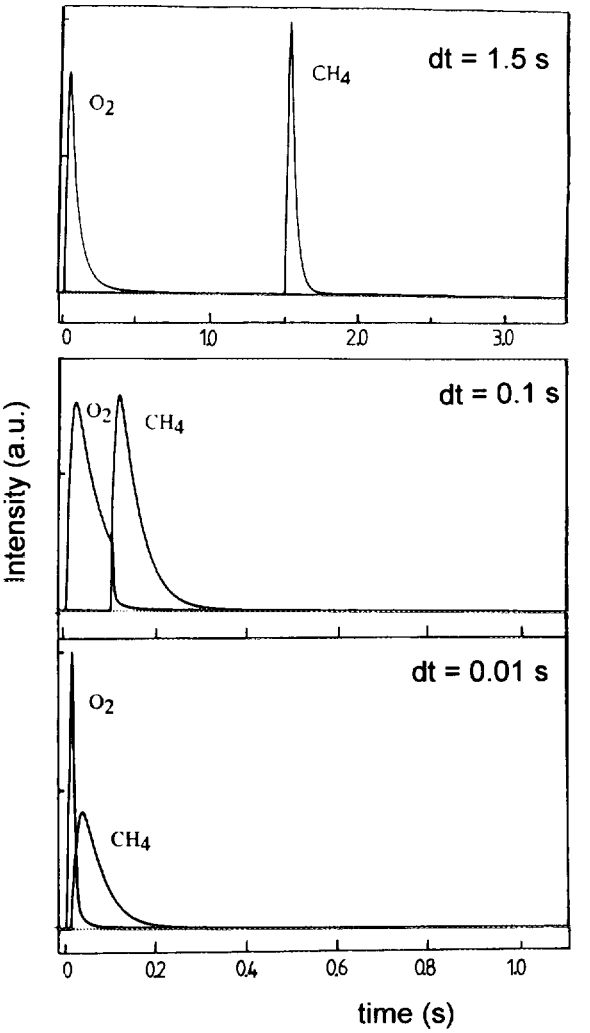

FIG. 9. TAP responses to sequential O_2 and CH_4 single pulses at 750°C for different time intervals between the pulses (C_2 and CO responses observed under methane pulses are not reported for sake of clarity).

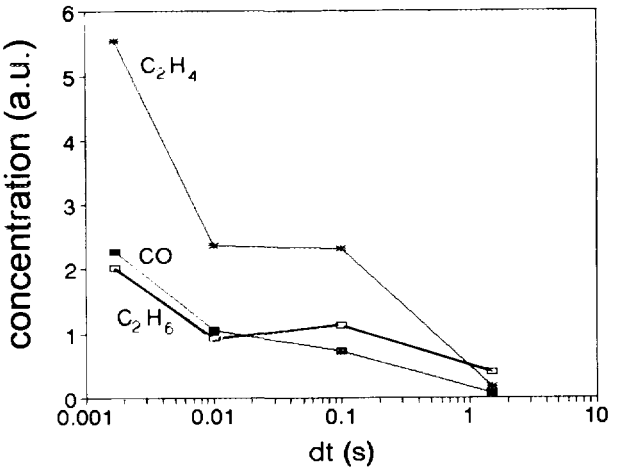

FIG. 10. Amount of C_2's and CO produced during sequential O_2 and CH_4 pulses (see Fig. 9) as a function of the time delay (*dt*) between O_2 and CH_4 pulses.

time interval (*dt*) between the two pulses was varied, as reported in Fig. 9. For each time interval the amount of products was evaluated, as reported in Fig. 10. The following features were revealed by these experiments:

(i) When the two CH_4 and O_2 pulses were not overlapping ($dt > 1$ s), each of them tended to be identical to single pulses of either oxygen or methane. Note that in this case only traces of OCM products were detected at the reactor outlet (Fig. 10),

(ii) When the CH_4 and O_2 pulse overlapped the O_2 pulse ($dt < 1$ s), oxygen was rapidly consumed and the methane peak decreased. In this case, significant amounts of OCM products were detected at the reactor outlet, but always at the same time as the methane signal. Note that CO_2 was never detected, probably due to readsorption effects. Similar results were reported for Sm_2O_3 (14) and Ba/Sr/Sm_2O_3 (13) catalysts.

(iii) The C_2 amount was a maximum when oxygen and methane were pulsed together, i.e., when the amount of gaseous oxygen in contact with methane was the highest. This important feature reveals that no delay (measurable by the TAP system) is required between oxygen activation and methane conversion.

Catalytic data obtained when single pulses of mixed methane, oxygen, and argon were admitted into the TAP reactor under a Knudsen or a non-Knudsen transport regime are reported in Table 4. Data obtained in a flow system operated at atmospheric pressure, i.e., under the viscous flow regime, are also reported for comparison at similar methane conversion level.

Under a Knudsen diffusion regime (i.e., without significant collisions in the gas phase), significant amounts of methyl radicals but only few C_2 products were detected at the TAP reactor outlet. Under an "intermediate" regime (where gas phase collisions started to occur), the concentration of evolving radicals was found to decrease while the selectivity to ethane increased markedly. In the dynamic flow reactor, i.e., under a purely viscous regime, a still larger selectivity to C_2 products was indeed observed.

Within the C_2 products, the absence of ethylene under the Knudsen regime (Table 4) proves that only ethane is a primary product; ethylene must be then considered as arising from a subsequent dehydrogenation of ethane, as generally proposed in the OCM literature.

DISCUSSION

Reversible activation of methane. No reversibly adsorbed methane was found to accumulate on the lanthana surface under reaction conditions. This important feature, also reported for other catalysts (11–14), rules out any mechanistic step based on a Langmuir–Hinshelwood model, which would assume an accumulation of adsorbed methane before a slow step of surface reaction. However, this result does not discard any kind of interaction between gas phase and surface, if it is fast enough or if the rate of desorption is close to the rate of adsorption, impeding surface accumulation. Actually, this corresponds typically to the interaction revealed by the isotopic exchange experiments.

Thus, the isotopic exchange occurring between cofed CH_4 and CD_4 clearly demonstrates that methane can be reversibly activated over lanthana catalysts, following a stepwise process. This property was already observed by Quanzhi and Amenomiya on alumina (29) and Buyevskaya *et al.* on samaria (14). It may more generally be related to former studies on CH_4/D_2 exchange carried out over oxide material (30, 31). For this case, it is generally agreed that the activation of methane proceeds via a heterolytic splitting of the C–H bond on a cation–anion pair Me^{n+}–O^{2-}, following

$$H_3C\text{–}H + Me^{n+}\text{–}O^{2-} \rightleftharpoons H_3C\text{–}Me^{(n-1)+}\text{–}OH^- . \quad [1]$$

The present study provides evidence of a strong inhibiting effect of CO_2 on the CH_4/CD_4 isotopic exchange. As deduced from FTIR studies (22, 32), the acidic molecule CO_2 interacts with the lanthana surface via basic lattice oxygen O^{2-} to form surface carbonate species under OCM conditions, following

$$CO_2 + (O^{2-}) \rightleftharpoons (CO_3^{2-}). \quad [2]$$

It may then be inferred that the reversible activation of methane proceeds mainly on the basic sites of the lanthana surface. This conclusion is in good keeping with a previous study carried out on a series of rare-earth

oxides, showing that the CH_4/CD_4 equilibration followed strictly the basicity of the oxides (considered in their highest possible oxidation state), ranked according to their ionic radius (26):

$$La > Gd > Ce > Sm > Pr > Ho > Tm.$$

To summarise, it is proposed that the reversible activation of methane occurs under OCM conditions via a heterolytic splitting on the surface basic pairs $\{La^{3+}, O^{2-}\}$, according to Eq. [1], replacing Me^{n+} with La^{3+}.

Irreversible activation of methane. The irreversible activation of methane, i.e., its transformation into OCM products, has been shown to be affected also by the presence of CO_2, but to a much lesser extent than the reversible activation. This suggests that both processes of reversible and irreversible activation of methane require basic sites but probably not in a similar way. In other words, if the reversible activation appears to be directly related to the surface basicity, the irreversible activation may depend on surface basicity through a more complex and less direct manner.

This distinct behaviour towards surface basicity between reversible and irreversible activation of methane raises now the question of whether the reversible activation precedes the step of the irreversible activation (consecutive reactions) or the two processes are independent, i.e., parallel.

Let us assume a consecutive process as depicted in Scheme 1:

$$CH_4 \rightleftharpoons CH_3^- + H^+$$
$$CH_3^- \rightarrow CH_3^{\cdot} + e^-$$

SCHEME 1

From the measurements of kinetic isotope effects, many authors concluded that the slow step of the route which transforms gaseous methane into ethane, i.e., the irreversible activation of methane, involved a homolytic C–H bond breaking into H and methyl radicals (17, 20, 21).

In the case of Scheme 1, there are two possibilities. (i) The slow step corresponds to the reversible formation of the CH_3^- carbanion, in agreement with the KIE effects. Within this assumption, the irreversible transformation of the carbanion into a methyl radical via electron transfer has to be considered as fast, which would displace the former equilibrium toward the right and therefore make the isotopic exchange unlikely, which was not observed. (ii) The slow step corresponds to the irreversible transformation of the carbanion. For this case, no isotopic effect is expected from an electron transfer, which does not correspond to the observed KIE. Furthermore, the isotopic exchange would remain the major reaction under OCM conditions, which again was not the case. Accordingly, Scheme 1 appears unlikely and two independent or parallel routes have to be considered for the two modes of methane activation, as depicted in Scheme 2:

$$CH_4 \begin{cases} \nearrow CH_3^- + H^+ & \text{reversible activation} \\ \searrow CH_3^{\cdot} + H^{\cdot} & \text{irreversible activation} \end{cases}$$

SCHEME 2

Following Scheme 2, the active sites corresponding to the two different routes are necessarily distinct. Concerning the reversible activation of methane, basic $\{La^{3+}, O^{2-}\}$ pairs were proposed above as active centres, irrespective of the absence or the presence of oxygen. Concerning the irreversible activation, it has been shown to occur only in the presence of oxygen. This statement strongly suggests that the related active centres are dealing with forms of activated oxygen, able to attack irreversibly the stable C–H bond of methane. The question arises now as to specify how oxygen activates under OCM conditions.

Oxygen activation. No oxygen uptake by the lanthana catalyst was observed by TAP experiments, whatever the temperature and the catalyst pretreatment are. At variance with that result, Statman *et al.* (13) observed that all the pulsed oxygen was adsorbed at 600°C on Ba/Sr/Sm_2O_3, while it was reported by Buyevskaya *et al.* (14) that only a small amount of oxygen was adsorbed on pure samaria under similar conditions. These distinct behaviours could reflect different densities of surface defects which may be filled with activated oxygen.

From the observation of a statistical equilibrium during the transient experiments switching from $^{16}O_2$ to $^{18}O_2$ (SSITK and TAP), it may be inferred that a fast gas phase/surface equilibrium involving a dissociative adsorption process takes place for oxygen under OCM conditions, without accumulation on the surface (as already discussed for the reversible activation of methane). This behaviour was also observed by Peil *et al.* (11) on Li/MgO and Ekstrom and Lapszewicz (12) on Sm_2O_3. Moreover, large and fast isotopic mixing of the lattice oxygen atoms, without surface enrichment, was shown to occur with the lanthanum oxide. This underlines the high lattice oxygen mobility and demonstrates that the gaseous oxygen activation proceeds dissociatively and involves lattice oxygen.

A pretreatment with CO_2, leading to the formation of surface carbonate (22), was found to inhibit markedly the oxygen reversible activation. This indicates that the O_2 activation involves the same basic sites as CO_2, although via a distinct process since the former leads to the dissoci-

ation of O_2, while the latter proceeds via an associative adsorption (Eq. [2]). Ito *et al.* (8) have proposed that the activation sites for oxygen on OCM catalysts could be O^{2-} atoms associated to surface anion vacancies, □, to give O^- adspecies, as follows:

$$1/2\ O_2 + \{O^{2-} + \square\} \rightleftharpoons 2(O^-). \quad [3]$$

This type of oxygen activation, combined with an equilibrium between surface species and bulk lattice atoms (Eq. [5]), perfectly accounts for the results of isotopic exchange reported above:

$$^{18}O_2 + 2\{^{16}O^{2-} + \square\} \rightleftharpoons 2(^{16}O^-) + (^{18}O^-)$$
$$\rightleftharpoons {}^{16}O^{18}O + \{^{16}O^{2-} + \square\} + \{^{18}O^{2-} + \square\} \quad [4]$$

$$\{^{18}O^{2-} + \square\} + [-{}^{16}O^{2-}-] \rightleftharpoons \{^{16}O^{2-} + \square\} + [-{}^{18}O^{2-}-]. \quad [5]$$

Although no *in situ* technique is able today to specify directly the actual nature of the activated oxygen species under the OCM conditions, Eq. [3]–[5] appear quite plausible for the following reasons:

(i) Equation [3] leads to the formation of an electrophilic surface oxygen which should be able to activate the C–H bond of methane into a methyl radical. Regarding the literature, the O^- species has never been detected on lanthana, even under conditions far from the OCM ones (at low temperature and pressure). This could be due to its very short lifetime, as shown by the TAP experiments. Actually, according to the energy diagram of oxygenated species in oxide materials proposed by Bielanski and Haber (33), O^- and O_2^-, the most stable adsorbed species, present close stabilisation energies. O_2^- has been detected on La_2O_3 by Wang and Lunsford (34) by EPR spectroscopy. Therefore the electrophilic site formed during O_2 adsorption could be O^- or O_2^-. Both species are very likely to be in equilibrium since they result from a series of equilibrated steps where oxygen is progressively enriched in electrons (33–35), according to

$$O_2\ \text{gas} \rightleftharpoons (O_2) \overset{e^-}{\rightleftharpoons} (O_2^-) \overset{2e^-}{\rightleftharpoons} 2(O^-). \quad [6]$$

(ii) Equations [3]–[5] involve surface vacancies which may be related to the surface defects well identified on lanthanum oxide. Grain boundaries have clearly been observed by electron microscopy in Part I of this work (22). They induce a tension between the crystallites which can be partly released by the creation of electronic vacancies. Hargreaves *et al.* (36) pointed out that these structural defects, observed after addition of lithium on magnesia, had a beneficial effect on the OCM performance.

Interaction between methane and oxygen. From the TAP experiments, the conversion of methane into C_2 products was found to be maximum when oxygen and methane were pulsed together, i.e., when the amount of gaseous oxygen in contact with methane was the highest. This important feature strengthens the idea that the adsorbed species resulting from the fast reversible oxygen activation are directly involved in the process of methyl radical generation. Thus, in the presence of methane, the (O^-) active species resulting from the equilibrium of Eq. [3] would also be involved in the irreversible step of methane activation. This new route which involves the consumption of (O^-) species would account for the marked decrease in the rate of oxygen isotopic exchange observed experimentally under OCM conditions. It can be written as originally proposed by Ito *et al.* (8):

$$CH_4 + (O^-) \rightarrow CH_3^{\cdot} + (OH^-). \quad [7]$$

The further surface dehydroxylation favoured by the high temperature would allow the regeneration of the site for oxygen activation:

$$2\,(OH^-) \rightarrow H_2O + \{O^{2-} + \square\}. \quad [8]$$

Ethane formation. The observation that the C_2 hydrocarbons and $CH_3^{\cdot}$ radical concentrations vary in a reverse direction (Table 4) reinforces the general assumption that ethane and ethylene derive from the coupling of methyl radicals. Furthermore, it was observed that this coupling is favoured when gas collisions are enhanced, i.e., for viscous transport regime. This result tends to demonstrate that the coupling of methyl radicals takes place in the gas phase and not on the surface, in agreement with the results of Feng *et al.* (7). However, it may be noted that the coupling of two methyl radicals on the surface would also be favoured when increasing the pulse intensity, due to a higher surface concentration, favouring the recombination. Therefore the latter hypothesis of surface coupling

TABLE 5

Surface Sites Involved in the OCM Process over Lanthana and the Resulting Intermediate Species

Reaction	Surface site	Intermediate species
CH_4 reversible activation	$\{O^{2-}, La^{3+}\}$	$CH_3^{\cdot}$, $H^{\cdot}$
O_2 reversible activation	$\{O^{2-}, \square\}$	(O^-) or (O_2^-)
CO_2 reversible adsorption	$\{O^{2-}\}$	(CO_3^{2-})
Methyl radical formation	(O^-) or (O_2^-)	$CH_3^{\cdot}$; OH^-
C_2H_6 dehydrogenation	(O^-) or (O_2^-)	$C_2H_5^{\cdot}$; OH^-
CO_2 formation	$\{O_{CUS}, \square\}$	(CH_3O^-)

cannot be totally ruled out on the basis of these experiments.

From the observation that ethylene is not produced in the case of Knudsen pulses while ethane starts to be formed (Table 4), it is confirmed that ethylene is a secondary product of the coupling reaction, most likely arising from the subsequent dehydrogenation of ethane. As discussed in Ref. (5), the latter is likely to involve ethyl radicals as intermediates, in a way similar to the irreversible activation of methane.

CO_2 formation. The specific methane oxidation to carbon dioxide was investigated in Part I of this study (22). The conclusion was that specific surface sites, associating low coordination (coordinatively unsaturated) lattice oxygen atoms with anion vacancies $\{O_{CUS}, \square\}$, were responsible for the total oxidation of methyl radicals through successive surface steps, involving O^- adspecies, at least under moderate OCM conditions ($T < 750$°C). This oxidation path would then be in competition with the selective route of methyl coupling.

Table 5 summarises the different types of active sites which have been proposed in the present study to account for the OCM reaction over lanthana catalysts.

CONCLUSIONS

A mechanistic scheme of the main heterogeneous steps of the OCM reaction has been proposed for the case of lanthana catalysts, specifying the nature of the sites involved in the selective and nonselective pathways. In reference to the mechanistic studies reported in the literature on other types of OCM catalyst, it is now obvious that no single and simple mechanism applies for this reaction, due to the intricate network of the elementary selective and nonselective steps. However, some general behaviour such as (i) the fast interaction between gaseous oxygen and lattice atoms, involving the formation of active surface species able to activate C–H bonds and (ii) the two parallel ways (reversible and irreversible) of methane activation could be considered for most of the performing systems.

ACKNOWLEDGMENTS

This work was supported by the European Community (Joule Programme—JOUF 0044-C). Thanks are due to Professor M. Baerns for welcoming S.L. in his laboratory and to Dr. G. A. Martin for helpful discussions.

REFERENCES

1. Lunsford, J. H., *in* "Methane Conversion by Oxidative Processes" (E. E. Wolf, Ed.), p. 3. Van Nostrand–Reinhold, New York, 1992.
2. Lunsford, J. H., *in* "New Frontiers in Catalysis" (L. Guczi et al., Eds.), Series A, p. 103. Elsevier, New York, 1993.
3. Sokolovskii, V. D., and Mamedov, E. A., *Catal. Today* **14,** 331 (1992).
4. Maitra, A. M., *Appl. Catal.* **104,** 11 (1993).
5. Martin, G. A., and Mirodatos, C., *Fuel Process. Technol.* **42,** 179 (1995).
6. Amorebieta, V. T., and Colussi, A. J., *J. Phys. Chem.* **92,** 4576 (1988).
7. Feng, Y., Niiranen, J., and Gutman, D., *J. Phys. Chem.* **95,** 6564 (1991).
8. Ito, T., Wang, J.-X., Lin, C.-H., and Lunsford, J. H., *J. Am. Chem. Soc.* **107,** 5062 (1985).
9. Choudhary, V. R., and Rane, V. H., *J. Catal.* **130,** 411 (1991); *J. Catal.* **135,** 310 (1992); *J. Chem. Soc. Faraday Trans.* **90,** 3357 (1994).
10. Ito, T., Watanabe, T., Tashiro, T., and Toi, K., *J. Chem. Soc. Faraday Trans.* **85,** 2381 (1989); Ito, T., Tashiro, T., Watanabe, T., Toi, K., and Kobayashi, H., *J. Phys. Chem.* **95,** 4476 (1991).
11. Peil, K. P., Goodwin, J. G., and Marcelin, G., *J. Phys. Chem.* **93,** 5977 (1989); *J. Am. Chem. Soc.* **112,** 6129 (1990); *J. Catal.* **131,** 143 (1991).
12. Ekstrom, A., and Lapszewicz, J. A., *J. Phys. Chem.* **93,** 5230 (1989); *J. Am. Chem. Soc.* **111,** 8515 (1989).
13. Statman, D. J., Gleaves, J. T., McNamara, D., Mills, P. L., Fornasari, G., and Ross, J. R. H., *Appl. Catal.* **77,** 45 (1991).
14. Buyevskaya, O. V., Rothaemel, M., Zanthoff, H., and Baerns, M., *J. Catal.* **146,** 346 (1994); **150,** 71 (1994).
15. Kalenik, Z., and Wolf, E. E., *Catal. Lett.* **9,** 441 (1991).
16. Campbell, K. D., and Lunsford, J. H., *J. Phys. Chem.* **92,** 5792 (1988).
17. Nelson, P. F., Lukey, C. A., and Cant, N. W., *J. Catal.* **120,** 216 (1989).
18. Nelson, P. F., and Lukey, C. A., *J. Phys. Chem.* **92,** 6176 (1988).
19. Mirodatos, C., Holmen, A., Mariscal, R., and Martin, G. A., *Catal. Today* **6,** 601 (1990).
20. Lehmann, L., and Baerns, M., *J. Catal.* **135,** 467 (1992).
21. Cant, N. W., Kennedy, M., and Nelson, P. F., *J. Phys. Chem.* **97,** 1445 (1993).
22. Lacombe, S., Geantet, C., and Mirodatos, C., *J. Catal.* **151,** 439 (1994).
23. Lin, C. H., Campbell, K. D., Wang, J. X., and Lunsford, J. H., *J. Phys. Chem.* **92,** 750 (1988).
24. Gleaves, J. T., Ebner, J. R., and Kuechler, T. C., *Catal. Rev. Sci. Eng.* **30,** 49 (1988).
25. Mirodatos, C., *J. Phys. Chem.* **90,** 481 (1986); *Catal. Today* **9,** 83 (1991); *in* "Catalyst Characterization" (B. Imelik and J. C. Védrine, Eds.), p. 651. Plenum Press, New York, 1994.
26. Lacombe, S., Holmen, A., Wolf, E. E., Ducarme, V., Moral, P., and Mirodatos, C., *in* "Natural Gas Conversion II: Proceedings, 3rd Natural Gas Conversion Symposium, Sydney, 1993," p. 211. Elsevier Amsterdam, 1994.
27. Mims, C. A., Hall, R. B., Rose, K. D., and Myers, G. R., *Catal. Lett.* **2,** 361 (1989).
28. Roos, J. A., Korf, S. J., Veehof, R. H. J., van Ommen, J. G., and Ross, J. R. H., *Appl. Catal.* **52,** 131 (1989).
29. Quanzhi, L., and Amenomiya, Y., *Appl. Catal.* **23,** 173 (1986).
30. Bird, R., Kemball, C., and Leach, H. F., *J. Catal.* **107,** 424 (1987).
31. Utiyama, M., Hattori, H., and Tanabe, K., *J. Catal.* **53,** 237 (1978).
32. Le Van, T., Che, M., Tatibouët, J. M., and Kermarec, M., *J. Catal.* **142,** 18 (1993).
33. Bielanski, A., and Haber, J., *Catal. Rev. Sci. Eng.* **19,** 1 (1979).
34. Wang, J.-X., and Lunsford, J. H., *J. Phys. Chem.* **90,** 3890 (1986).
35. Dubois, J. L., Bisiaux, M., Mimoun, H., and Cameron, C. J., *Chem. Lett.* 967 (1990).
36. Hargreaves, J. S. J., Hutchings, G. J., Joyner, R. W., and Kiely, C. J., *Catal. Today* **10,** 259 (1991).